IEEE Access
Multidisciplinary | Rapid Review | Open Access Journal

Received March 1, 2020, accepted March 17, 2020, date of publication March 20, 2020, date of current version April 1, 2020.

Digital Object Identifier 10.1109/ACCESS.2020.2982213

Gearbox Incipient Fault Detection Based on Deep Recursive Dynamic Principal Component Analysis

HUAITAO SHI[1], JIN GUO[1], XIAOTIAN BAI[1], LEI GUO[1], ZHENPENG LIU[1], AND JIE SUN[2]
[1]School of Mechanical Engineering, Shenyang Jianzhu University, Shenyang 110168, China
[2]State Key Laboratory of Rolling and Automation, Northeastern University, Shenyang 110819, China

Corresponding author: Xiaotian Bai (baixt@sjzu.edu.cn)

This work was supported in part by the National Key Research and Development Plan of China under Grant 2017YFC0703903, and in part by the National Science Foundation of China under Grant 51705341, Grant 51905357, and Grant 51675353.

ABSTRACT As a part of the energy transmission chain, gearboxes are considered as important components in rotating machines, and the gearbox failure results in costly economic losses. Therefore, it is necessary to detect the appearance of incipient gearbox faults by implementing an appropriate detected model. The incipient failure characteristics of the gearbox are weak and hidden in a set of time-varying series signals the vibration signals, which is difficult to effectively extract under the background of strong noise. The PCA method is not effective in detecting weak fault features in time-varying signals, so this paper proposes a method based on Deep Recursive Dynamic Principal Component Analysis (Deep RDPCA) to detect incipient faults in gearboxes. The proposed approach is modeled via both the deep decomposed theorems and time-varying dynamic model based on traditional PCA to extract characteristic of time-varying and weak fault information under the background of strong noise. The proposed method could get a better real-time reflection for changed system by introducing ''Moving Window'' technologies, so that the incipient fault of gearbox could be detected accurately, too. Finally, the effect of Deep RDPCA-based fault diagnosis is compared with the results of PCA, DPCA, RDPCA, Deep PCA, and Deep DPCA methods. It is concluded that the proposed method can effectively capture the time-varying relationship of process variables and accurately extract the weak fault characteristics in the vibration signal, which effectively improves the fault detection performance.

INDEX TERMS Gearbox, fault diagnosis, gear failure experiment, feature extraction, Deep RDPCA.

I. INTRODUCTION

Gearbox is the key component of mechanical transmission and plays an important role in the transmission system [1]–[3]. The internal structure of gear box is compact and there are strong coupling effects between the components, which can easily cause gear pitting and broken teeth [4], [5]. Compared with other components, the maintenance of gearbox is more complicated and maintenance time is longer, which leads to great economic losses. Therefore, it is of great significance to identify the weak fault features at an incipient stage before the fault develops to a serious degree. Incipient fault detection is important to ensure the normal operation of equipment and avoid economic losses [6]–[8].

The incipient failure features of the gearbox can be described as following [9], [10]: (1) The dynamic response is not obvious due to the weak fault. (2) Signal modulation appears under the influence of multiple gear meshes. (3) The transmission path of the gearbox vibration signal is complicated, which lowers the signal-to-noise ratio with the effect of excessive noise. (4) The fault characteristics vary with time, and it is difficult to identify the fault condition. Therefore, how to extract incipient fault characteristic from weak signals that have been flooded by noise is the key to incipient fault detection [11].

The model-based method is one of the early fault detection methods for gearboxes, which requires accurate prior physical models of gears [12]–[15]. However, the motions and internal forces in the gearbox are complicated, which reduces the model accuracy and extends the calculation time. Signal processing is also a common early-stage fault detection method [16]–[17] such as, the empirical mode decomposition method [18] and wavelet transform method [19]. The feature extraction process contains some redundant

The associate editor coordinating the review of this manuscript and approving it for publication was Yan-Jun Liu.

information, the data dimension is high and the calculation efficiency is low, too. Incipient fault detection methods based on deep learning can compress signals [20]–[24] and reduce the data dimension. But the computational intensity of its model becomes larger, and the training speed of the system decreases in large network structures.

During the actual operation of the gearbox, the variables are driven by random noise and uncontrollable interference, and show a certain degree of autocorrelation, which affects the detection results of failures [25], [26]. Qin proposed an incipient fault detection method based on Deep PCA [27] which can accurately extract weak fault features and detect the incipient faults. Deep PCA is mainly a diagnostic method for the control process, which cannot extract and process vibration signals of mechanical equipment to diagnose faults. Meanwhile, Deep PCA ignores the time-varying feature of the vibration signals in the actual process, which reduces the performance of fault detection. Many scholars have proposed various methods for time-varying feature [28], [29]. Tang use the time-varying barrier Lyapunov function to model the dynamic system [30]. Ku proposed dynamic PCA to delay variables into the data array to construct a time-varying data array, thereby extracting time-varying and eliminating data sequence correlations [31].

The characteristics of the incipient faults are not obvious, and it is hard to extract from excessive noise. This paper proposes a dynamic incipient fault detection method based on Deep Recursive Dynamic Principal Component Analysis (Deep RDPCA) combined with the Moving Window algorithm. The main steps of Deep RDPCA method are as follow: (1) Transform the observation matrix into an augmentation matrix. (2) Update the latest samples to the augmented matrix, discard the oldest samples, and retain a fixed number of samples in the augmented matrix. (3) Decompose the updated matrix into multiple subspaces for detection and fully mine the fault information. On this basis, the algorithm is improved, and a simplified recursive formula of the autocorrelation matrix is given. The original fourth rank one modifications are simplified to two rank one modifications, which improves the online update speed.

This paper is mainly divided into following parts. The basic theoretical knowledge are introduced in the second part. A complex nonlinear dynamic process monitoring method for gearboxes based on Deep RDPCA is proposed in the third part. The performance of the scheme are verified through simulation experiments using incipient fault data in the fourth part. The proposed Deep RDPCA fault detection methods is summarized in the fifth part.

II. FUNDAMENTAL THEORY

A. DPCA METHOD

The DPCA fault detection method adds variables to the data matrix to construct a time lag matrix, and then improves the PCA to extract time-varying relationships, eliminate correlation of data sequences, and improve fault detection performance [32]. The steps of the DPCA method are as follows:

Give a training set $\mathrm{X} = [x_1^T, x_2^T, \cdots x_n^T]$,$x_i \in R^m$ n is the number of observed value, and m is the number of process variables.

Step 1: Standardize the training set.

Step 2: Choose S, devoting to extend into an augmented data matrix using the previous S observations.

$$X_S = \begin{bmatrix} x_t^T & x_{t-1}^T & \cdots & x_{t-S}^T \\ x_{t-1}^T & x_{t-2}^T & \cdots & x_{t-S-1}^T \\ \cdots & \cdots & \cdots & \cdots \\ x_{t+S-n}^T & x_{t+S-n+1}^T & \cdots & x_{t-n}^T \end{bmatrix} \tag{1}$$

Step 3: Compute the covariance matrix of augmented data matrix and eigenvalues are decomposed.

$$C = \frac{1}{n-1} (X_S)^T \mathrm{X}_S = V \Sigma V^T \tag{2}$$

where diagonal matrix $\sum$ contains the non-negative real eigenvalues of decreasing magnitude ($\lambda_1 > \lambda_2 > \cdots > \lambda_n$),V is eigenvector corresponding to the eigenvalues.

Step 4: Use the Cumulative Percentage Variance (CPV) to extract the principal component, a is the number of principal component.

$$CPV = \left[\frac{\sum_{i=1}^{a} \lambda_i}{\sum_{i=1}^{n} \lambda_i} \right] \times 100\% < 85\% \tag{3}$$

Step 5: Select load matrix $P \in R^{m \times a}$, The original space is divided into principal component subspace X_{S11} and residual subspace X_{S12}.

$$X_S = X_{S11} + X_{S12} = TP^T + X_{S12} \tag{4}$$

Step 6: Calculate the statistics of T^2 and SPE:

$$T^2 = X^T P \Lambda^{-1} P^T X \tag{5}$$

$$SPE = \left\| \left(I - PP^T \right) X \right\|^2 \tag{6}$$

where Λ is the principal component space characteristic value matrix.

Step 7: Calculate the control limit of T^2 and SPE:

T^2 satisfies the F distribution, and its control limit is:

$$T^2 \sim \frac{a(n^2-1)}{n(n-a)} F_{a,n-a} \tag{7}$$

Q satisfies the χ^2 distribution, and its control limit is:

$$\delta^2 = g\chi^2(h) \tag{8}$$

where, $g = {\rho^2}/{2\mu}$, $h = {2\mu^2}/{\rho^2}$. μ and ρ^2 is the mean and variance of SPE.

The specific process based on DPCA is shown in Fig.1:

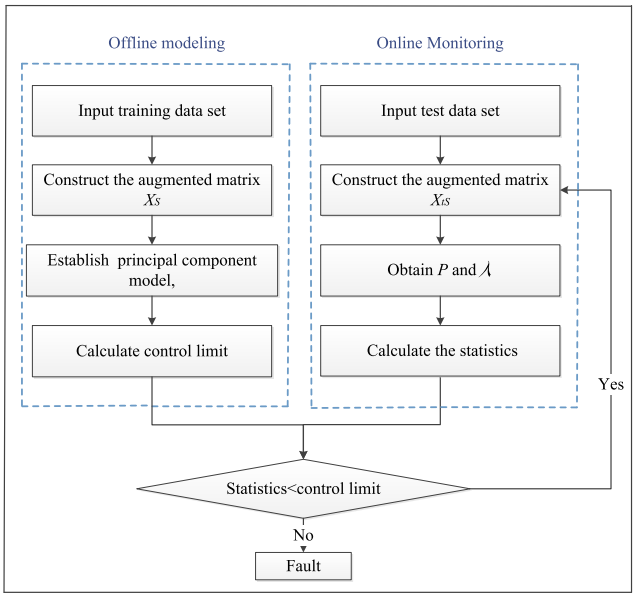

FIGURE 1. The process of DPCA.

B. DEEP DPCA METHOD

Due to some fault features will be discarded during the extraction of the principals, which may cause DPCA to fail to accurately detect weak initial fault information. Combined with the linear projection method, the Deep DPCA method is proposed. Deep DPCA method decomposes the data set into multiple data processing layers and retains more variance information. At the same time, the Deep DPCA method can effectively reveal the weak information hidden in the original data set.

Deep DPCA method has following advantages: (1) Effectively extract weak fault information in the data set. (2) Established accurate mathematical model. (3) Simple calculation and easy implementation.(4) It has excellent incipient fault detection performance. The steps of Deep DPCA method are as follow:

Step 1: Collect the vibration data X and standardize X.

Step 2: Select the appropriate the time lag S, and building augment matrixX_S◦

Step 3: Obtain the principal element space and the residual space of data set X_S by DPCA method:

$$X_S = X_{S11} + X_{S12} \tag{9}$$

where, X_{S11} is the first order principal component subspace of augment matrix X_S; X_{S12} is the first order residual subspace of augment matrix X_S. They can be obtained by:

$$\begin{aligned} X_{S11} &= P_{11}P_{11}^T X_S \\ X_{S12} &= (I - P_{11}P_{11}^T)X_S \end{aligned} \tag{10}$$

To obtain more information about the second order principal component space and residual space. We repeat the above process, then obtain that:

$$\begin{aligned} X_{S11} &= X_{S21} + X_{S22} \\ X_{S12} &= X_{S23} + X_{S24} \end{aligned} \tag{11}$$

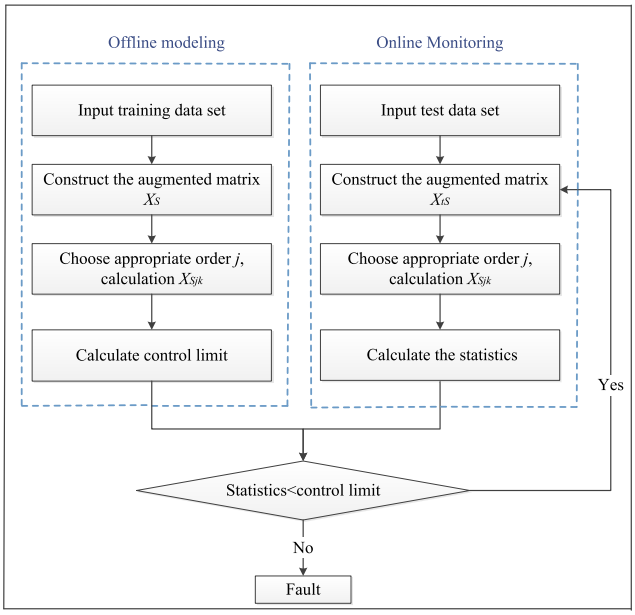

FIGURE 2. The process of deep DPCA.

Suppose P_{21} and P_{23} respectively are the principal vector of X_{S11} and X_{S12}; P_{22} and P_{24} respectively are the residual vector of X_{S11} and X_{S12}. Then the original data X can be obtained by:

$$X_S = X_{S11} + X_{S12} = X_{S21} + X_{S22} + X_{S23} + X_{S24} \tag{12}$$

where,

$$\begin{aligned} X_{S21} &= P_{21}P_{21}^T X_{S11} \\ X_{S22} &= (I - P_{21}P_{21}^T)X_{S11} \\ X_{S23} &= P_{23}P_{23}^T X_{S12} \\ X_{S24} &= (I - P_{23}P_{23}^T)X_{S12} \end{aligned} \tag{13}$$

By parity of reasoning, the augment matrix X_S can be represented as the sum of 2^j subspace, and j is the order. The subspace X_{Sjk} can be expressed as:

$$X_{Sjk} = \begin{cases} P_{jk}P_{jk}^T X_{Sj-1(k+1)/2} & k \text{ is odd} \\ \left(I - P_{jk-1}{P_{jk-1}}^T\right) X_{Sj-1\frac{k}{2}} & k \text{ is even} \end{cases} \tag{14}$$

where I is the identity matrix Suppose X_{Sjk} is the kth subspace of jth order,then $X_S = \sum_{k=1}^{2^j} X_{Sjk}$.

Next steps are similar to DPCA method. The specific process based on Deep DPCA is shown in Fig. 2:

III. DEEP RDPCA METHOD

Most practical industrial processes are time-varying, and their failure characteristics are weak for the incipient failures [33]. Incipient fault signals can be detected by Deep DPCA method, but the fixed control limit to monitor the time-varying system inevitably produce a certain false alarm rate. This paper proposes a new method based on the Deep Recursive Dynamic Principal Component Analysis (Deep RDPCA) for real-time monitoring of non-linear dynamic processes.

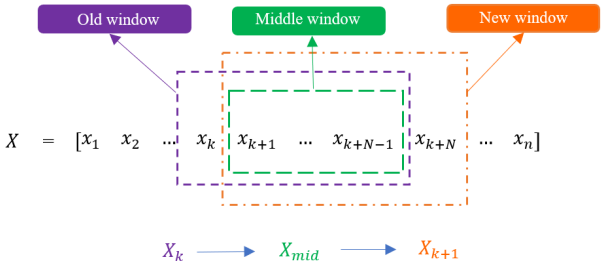

FIGURE 3. The adaptive update algorithm process.

A. MODEL UPDATE

In view of the time-varying relationship of the data, the data model is adaptively updated by combining "Moving Window" technologies [34]. It enables the principal component model to understand the changes of the system in real time, has certain timing-related characteristics, and guarantees that the length of the window does not change. N is the size of moving window, X_k is the k-th moving window matrix, X_{k+1} is the (k+1)-th moving window matrix, X_{mid} is the overlap of X_k and X_{k+1} The adaptive update algorithm process is shown in Fig. 3:

$S+1$ new data are used to construct an augmented data matrix, and adaptive moving windows is 1 in this paper, the covariance matrix is updated once when each $S+1$ sampling values is recurred. Assuming that the mean $\overline{X}_k$ and variance C_K of X_k are known, x^0_{k+1} is the normalized x_k so RPCA recurrence updating formula of data block can be simplified as:

$$\overline{X}_{k+1} = \frac{k}{k+1}\overline{X}_k + \frac{1}{k+1}x^0_{k+1} \tag{15}$$

$$X_{k+1} = [X_k \sum\nolimits_k \sum\nolimits^{-1}_{k+1} - 1_k \Delta\overline{X}_{k+1}{}^T \sum\nolimits^{-1}_{k+1} x^T_{k+1}]^T \tag{16}$$

$$C_{k+1} = \frac{k-1}{k}C_k + \frac{1}{k}x_{k+1}x^T_{k+1} + \sum\nolimits^{-1}_{k+1}\Delta\overline{x}_{k+1}\Delta\overline{x}^T_{k+1}\sum_{k+1}^{-1} \tag{17}$$

Update the first step of adaptive moving windows, the updating model is as follows:

$$\overline{X}_{mid} = \frac{N}{N-1}\overline{X}_k - \frac{1}{N-1}x^0_{k-N+1} \tag{18}$$

$$C_{mid} = \frac{N-1}{N-2}(C_k - \frac{1}{N-1}x_{k-N+1}x^T_{k-N+1} - \sum\nolimits^{-1}_{k-N+1}\Delta\overline{X}_{midk}\Delta\overline{X}_{midk}{}^T\sum\nolimits^{-1}_{k-N+1} \tag{19}$$

where $\Delta\overline{X}_{midk} = \overline{X}_k - \overline{X}_{mid}$, update the second step of adaptive moving windows:

$$\overline{X}_{k+1} = \frac{N-1}{N}\overline{X}_{mid} + \frac{1}{N}x^0_{k+1} \tag{20}$$

$$C_{k+1} = \frac{N-2}{N-1}C_{mid} + \frac{1}{N-1}x_{k+1}x^T_{k+1} + \sum\nolimits^{-1}_{k+1}\Delta\overline{X}_{mid(k+1)}\Delta\overline{X}_{mid(k+1)}{}^T\sum\nolimits^{-1}_{k+1} \tag{21}$$

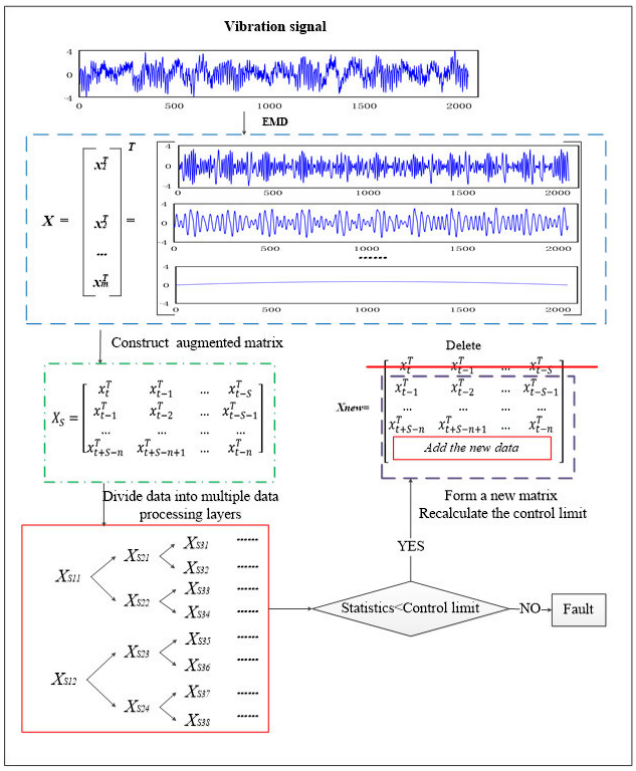

FIGURE 4. The structure of deep RDPCA.

where $\Delta\overline{X}_{mid(k+1)} = \overline{X}_{k+1} - \overline{X}_{mid}$. Substitute Eq.(15) into Eq.(17):

$$C_{k+1} = C_k - \frac{1}{N-1}x_{k-N+1}x^T_{k-N+1} - \sum\nolimits^{-1}_{k-N+1}\Delta\overline{X}_{midk}\Delta\overline{X}_{midk}{}^T\sum\nolimits^{-1}_{k-N+1} + \frac{1}{N-1}x_{k+1}x_{k+1}{}^T + \sum\nolimits^{-1}_{k+1}\Delta\overline{X}_{mid(k+1)}\Delta X^T_{mid(k+1)}\sum\nolimits^{-1}_{k+1} \tag{22}$$

According to the above formula, updating covariance avoid calculation of a big block matrix and complexity time-consuming of multiplication of matrices, however, it need to 4 times rank-one modification. In order to improve the online update rate rapidly

$$\sum\nolimits^{-1}_{k-N+1}\Delta\overline{X}_{midk}\Delta\overline{X}_{midk}{}^T\sum\nolimits^{-1}_{k-N+1} = \frac{1}{N^2}x_{k-N+1}x^T_{k-N+1} \tag{23}$$

$$\sum\nolimits^{-1}_{k+1}\Delta\overline{X}_{mid(k+1)}\Delta\overline{X}_{mid(k+1)}{}^T\sum\nolimits^{-1}_{k+1} = \frac{1}{N^2}x_{k+1}x^T_{k+1} \tag{24}$$

Leading (19) and (20) into (18):

$$C_{k+1} = C_k + \frac{N^2+N-1}{N^2(N-1)}(x_{k+1}x^T_{k+1} - x_{k-N+1}x^T_{k-N+1}) \tag{25}$$

The structure of Deep RDPCA incipient fault detection method is shown in Fig. 4:

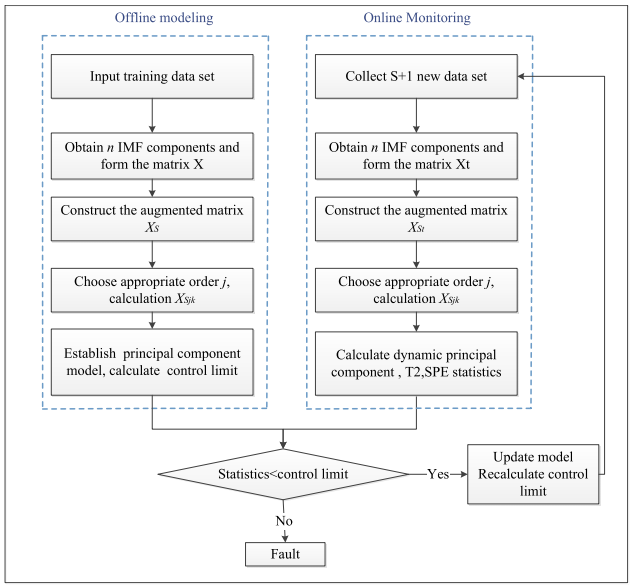

FIGURE 5. The process of deep RDPCA.

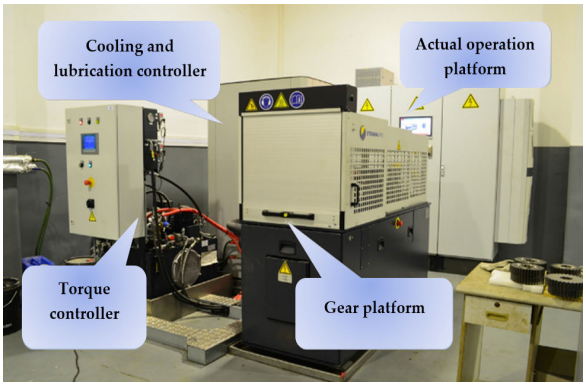

FIGURE 6. The gear fatigue test bench.

B. THE STEPS OF DEEP RDPCA

The fault diagnosis method of Deep RDPCA is divided into two parts: offline modeling and real-time online monitoring. First, collect a large amount of normal data, determine S, and use Deep DPCA to establish the initial model to obtain the appropriate control limit. Then, as each new sampling value of $S+1$ is collected, the observation value of the amplified data is reconstructed. Calculate its statistics and determine if it is fault data. The specific offline training and online diagnosis implementation steps are as follows:

a: OFFLINE MODELING

The method steps of offline modeling are as follows:

Step1: Collect vibration signals under normal conditions

Step2: Decompose the vibration signal by the EMD method to obtain m IMF components and the remaining terms Rn.

Step3: Compose m IMF components to a new matrix X and standardize X.

Step4: Determine S and extend the data set to the augment matrix X_S.

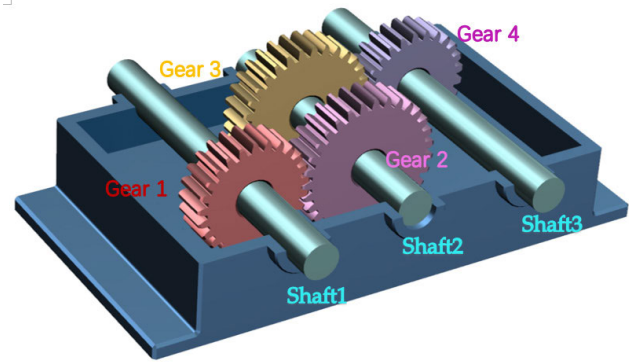

FIGURE 7. The internal structure of gearbox.

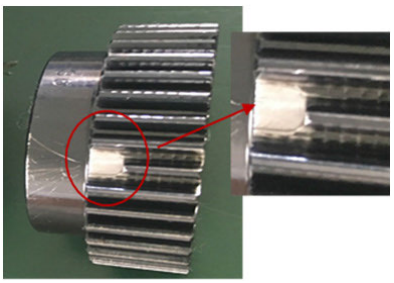

FIGURE 8. Broken tooth fault of gear.

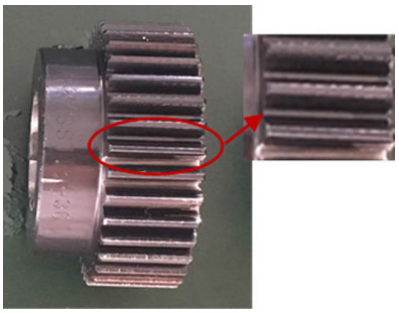

FIGURE 9. Pitting fault of gear.

Step5: Select the appropriate order j, and calculate the corresponding X_{Sjk} according to formula (14)

Step6: Calculate the number of principal component of each X_{Sjk}, the eigenvalue matrix Λ_{jk}, and the eigenvector matrix P_{jk}.

Step7: Calculate the control limits $TUCL_{jk}$ and $QUCL_{jk}$.

b: ONLINE MONITORING

The specific steps for online monitoring are as follows:

Step1: Collect $S+1$ vibration data set.

Step2: Decompose the vibration signal by the EMD method to obtain m IMF components and the remaining terms Rn.

Step3: Compose m IMF components to a new matrix X_t and standardize X_t.

Step4: Determine S and extend the data set to the augment matrix X_{St}.

Step5: Calculate the corresponding X_{Stjk} according to formula (14).

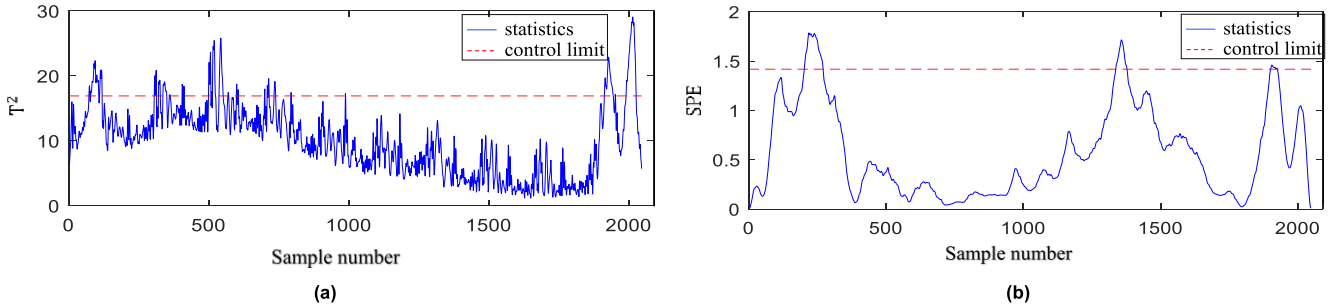

FIGURE 10. Experimental results of PCA fault detection method for broken tooth faults.

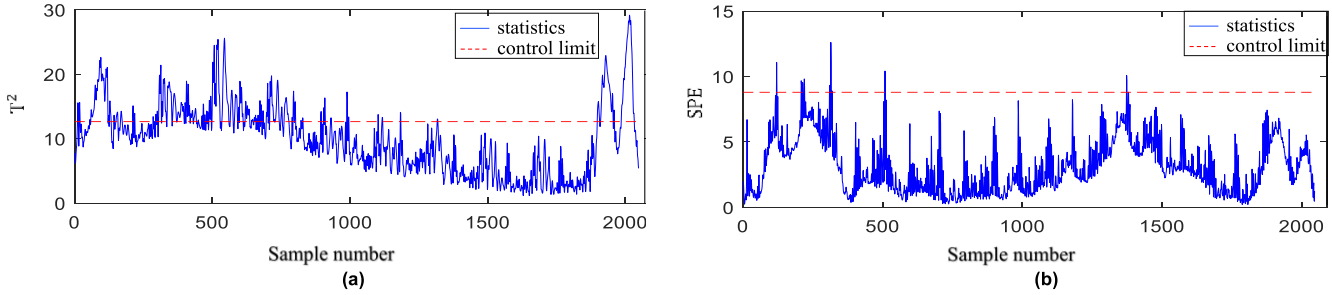

FIGURE 11. Experimental results of DPCA fault detection method for broken tooth faults.

Step6: Obtain the statistics T_{jk}^2 and SPE_{jk}.

Step7: Compare the obtained statistic with the corresponding control limit. If the statistic is greater than the control limit, a failure occurs. Otherwise, the data is in a normal state,then the new observation data is used to replace the old observation data, recalculate the dynamic principal component model, update control limits.

Fig. 5 depicts a flowchart of the fault detection method based on Deep RDPCA:

IV. EXPERIMENTAL RESULTS AND ANALYSIS

In this section, the full life cycle data of gear pitting and broken teeth collected by the gear fatigue test bench are used for experiments. Gear fatigue test bench shown in Fig. 6. Fig. 7 describes the internal structure of gearbox, and gear 3 is the position of the faulty gear. There are four gears in the gear box, the number of teeth is 31, 25, 25, 31. The driving shaft is shaft 1 and the driven shafts are shaft 2 and shaft 3.

Three groups of data with healthy gears, broken teeth fault and pitting fault were collected in the experiment. For the faults of broken teeth and pitting, the faulty gear is located at gear 3 in Fig.7. The broken teeth gear is shown in Fig. 8 and the pitting fault gear is shown in Fig. 9. Broken tooth fault was collected during the last 400 minutes of the full life cycle; pitting fault was collected during the last 600 minutes of the full life cycle. The gear materials of the two experiments are 40Cr, the rotation speed is 500r / min, the torque is 1400N*m. This section uses the 80th group of the two types of faults in the full life cycle for experiments. The fault characteristics of the fault data at this stage are weak, and the fault at this time is in the incipient stage. The vibration signal collected during the operation of the gearbox reflects the change of the gear with the running time. This time-varying characteristic is an important feature. The experimental analysis uses the missed detection rate and detection delay as the evaluation indicators of early fault detection performance.

A. GEARBOX BROKEN TEETH FAULT SIMULATION EXPERIMENT AND ANALYSIS

1) GEARBOX BROKEN TEETH FAULT SIMULATION EXPERIMENT

Gearbox broken teeth fault is one of common gearbox failure [37], [38]. Breaking of gear teeth usually occurs at the root of the gear because the bending stress at the root of the tooth is the largest. There are two main cases of broken teeth:

(1) Fatigue broken teeth: Because the bending stress generated by the root of the gear under load is a pulsating cyclic alternating stress, the combined effects of stress concentration sources such as machining tool marks and material defects will cause fatigue cracks. The cracks gradually spread and propagate, eventually leading to fatigue and broken teeth.

(2) Overload broken teeth: For gearboxes made of brittle materials such as cast iron or high-hardness alloy steel, due to severe overload or impact load, the stress on the dangerous section of the tooth root will exceed the limit value and the teeth will suddenly break.

Broken teeth of the gearbox makes the torque transmission unstable and produce impacts [37]. Such shocks will cause the fracture of other gear teeth and affect the service life of the gearbox. At the same time, the impact will also affect the accuracy and life of the gearbox shaft. Affects the reliability of the entire equipment operation and the normal operation of the equipment. In this section, a simulation experiment

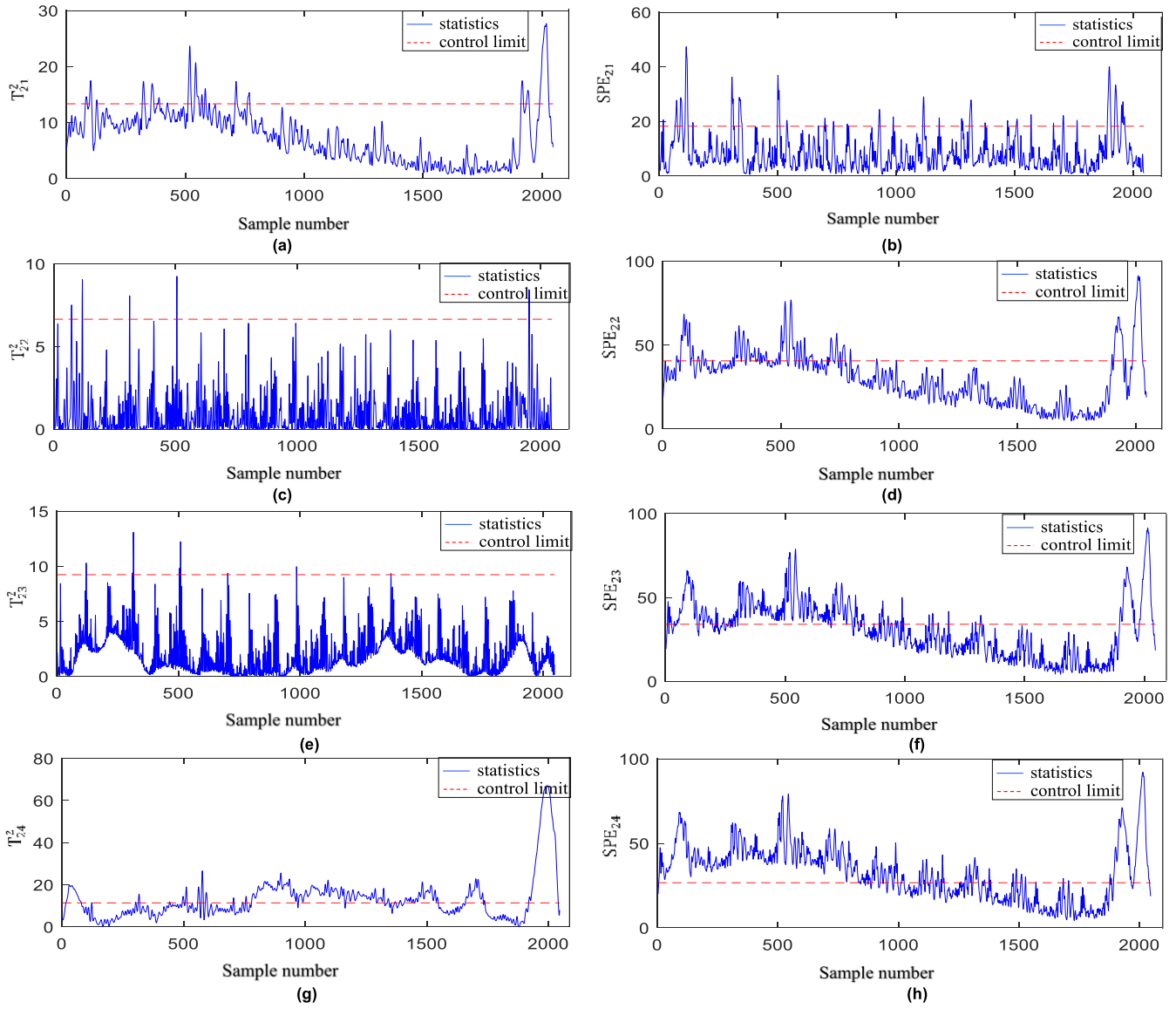

FIGURE 12. Experimental results of deep PCA fault detection method for broken tooth faults.

is performed on the gearbox with broken teeth. The specific results are as follows:

Fig. 10 and Fig.11 illustrate the results of traditional PCA fault detection methods and DPCA fault detection methods on broken tooth faults. Among them, Fig. 10 (a) and Fig. 11(a) describe the results of the T^2 statistic detection, and Fig. 10(b) and Fig(b) describe the results of the SPE statistics detection. In the figures, the solid blue lines represent statistics, and the red dashed lines represent control limits. It can be known from the simulation results that the traditional fault detection method can hardly detect the broken tooth fault.

Fig. 12 (a)-(h) respectively describe the T^2 and SPE fault detection results of the third layer data set $X_{21} - X_{24}$ of gear tooth broken, based on Deep PCA method. Fig. 13 (a)-(h) respectively describe the T^2 and SPE fault detection results of the third layer data set $X_{21} - X_{24}$ of gear tooth broken, based on Deep DPCA method. It can be seen from the simulation results that these two methods have certain incipient fault detection capabilities, and the fault detection effect of Deep DPCA is better than that of Deep PCA.

Fig. 14 illustrate the T^2 and SPE fault detection result of the broken tooth fault based on Deep RDPCA fault detection method. Among them, Fig. 14(a) and Fig. 14(b) illustrate the detection result of the first layer data set X_{01}. Fig. 14(c)-(f) describe the result of the second layer data sets data set X_{11} and X_{12}. Fig. 14(g)-(n) describe the third layer data sets $X_{21} - X_{24}$. The reduction in the number of samples on the abscissa is due to the moving window size of update model is 3, that is, every three sampling points obtain one result. So the final result is 1/3 of the initial number of samples. When the statistic exceeds the control limit, it indicates that the data is detected as faulty. From Fig. 14(a) and (b), we obtain that T^2_{01} and SPE_{01} are less affected by this fault; In the Fig. 14 (f), the impact of SPE_{12} by this fault is more

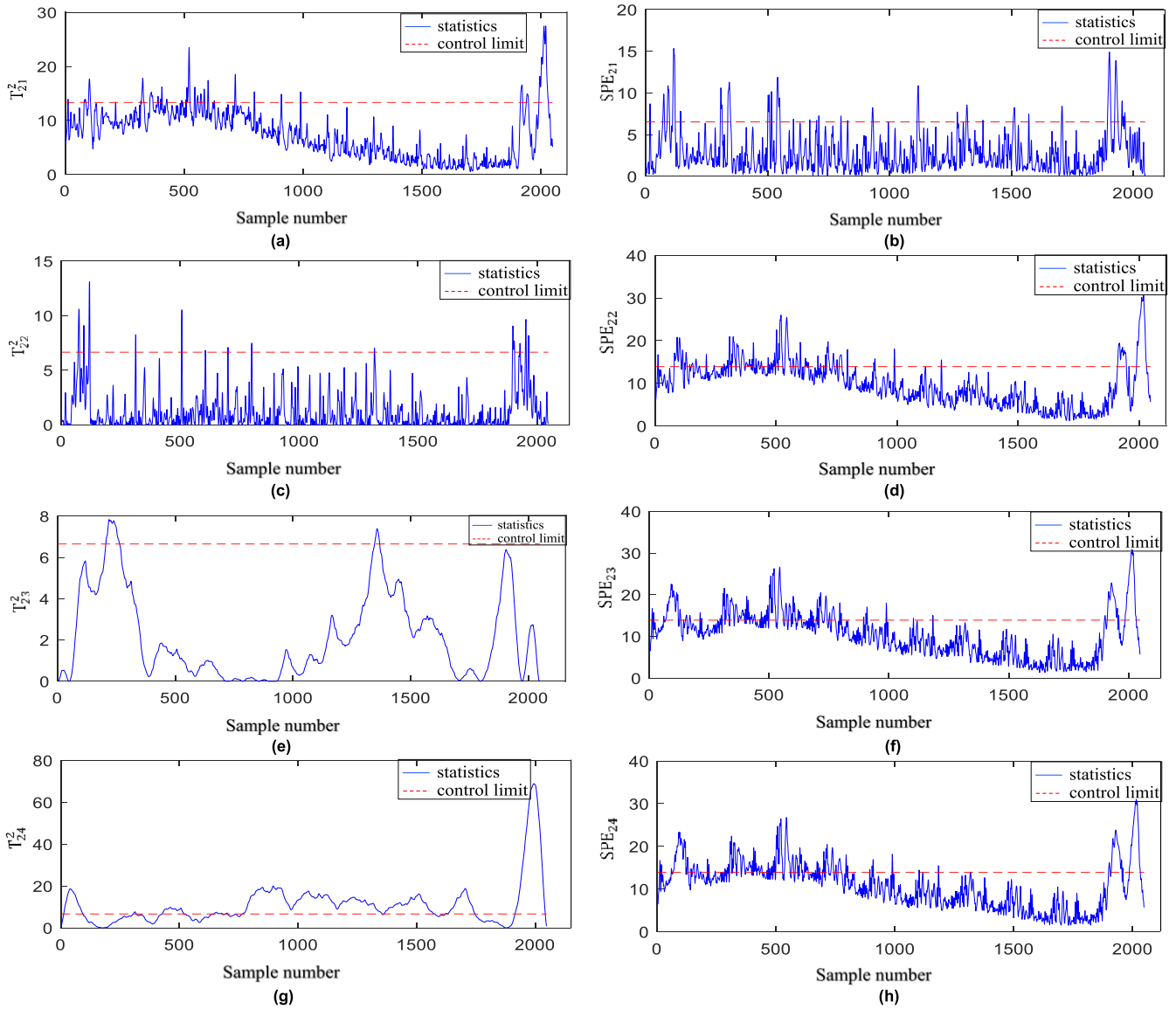

FIGURE 13. Experimental results of deep DPCA fault detection method for broken tooth faults.

obvious, other statistics are less affected by this fault; In the Fig. 14 (l) and (h), SPE_{23} and SPE_{24} are more affected by this fault. Therefore, the fault detection effect of the third-layer Deep RDPCA is better, which proves that the method has better incipient fault detection capability.

2) PERFORMANCE COMPARISON

This part compares the experimental results of PCA, DPCA, RDPCA, Deep PCA, Deep DPCA, and Deep RDPCA by analyzing the missed detection rate and detection delay of the gearbox broken tooth experiment results.

Table 1 describes the performance comparison of six methods for gearbox broken teeth. From the perspective of missed diagnosis rate, the PCA, DPCA and RDPCA method have a missed detection rate about 80%. These three methods basically do not have the capability of incipient failure detection. The missed detection rate of Deep PCA and Deep DPCA are significantly reduced, which can basically detect incipient failures. At the same time, compared with these two methods, the fault detection effect of Deep DPCA is better than that of Deep PCA. This is because Deep DPCA considers the time-varying of data. The missed detection rate of Deep RDPCA proposed in this paper is 16.73%, and the effect is the best.

From the perspective of detection delay, the PCA method detects a failure at the 101st sampling point. The DPCA method detects ruler failure at the 94th sampling point.

TABLE 1. Gearbox broken teeth fault performance comparison.

Detection method	missed detection rate	detection delay
PCA	85.46%	101
DPCA	81.37%	94
RDPCA	79.15%	87
Deep PCA	29.88%	31
Deep DPCA	24.34%	28
Deep RDPCA	16.73%	24

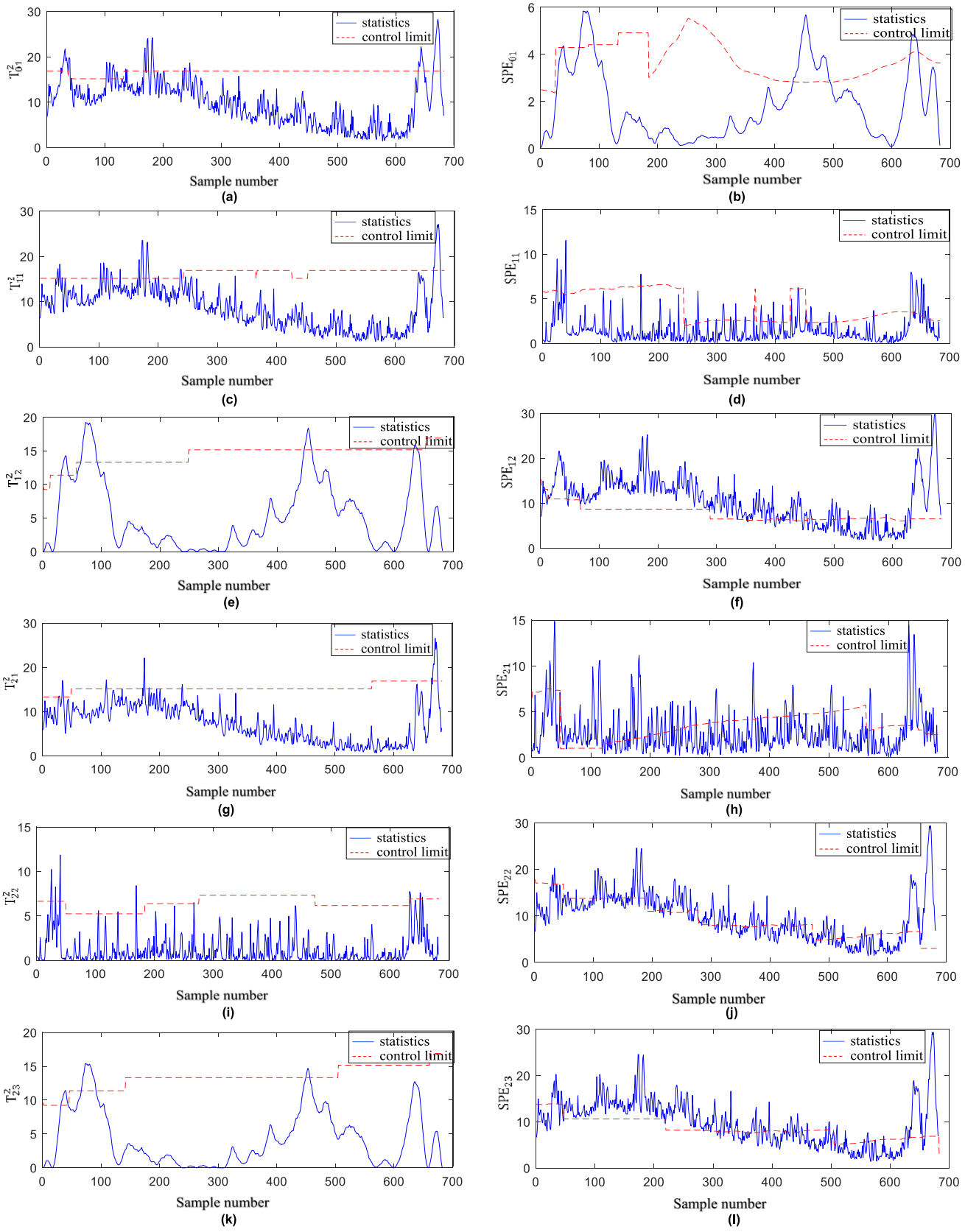

FIGURE 14. Experimental results of deep RDPCA fault detection method for broken tooth faults.

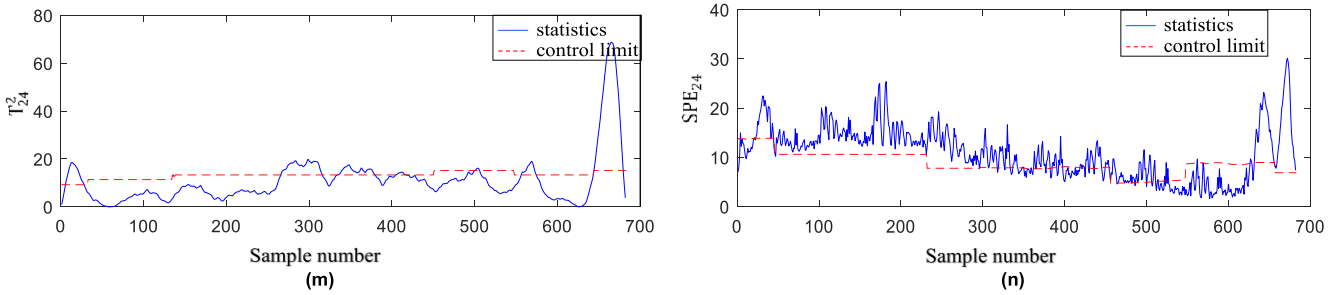

FIGURE 14. *(Continued.)* **Experimental results of deep RDPCA fault detection method for broken tooth faults.**

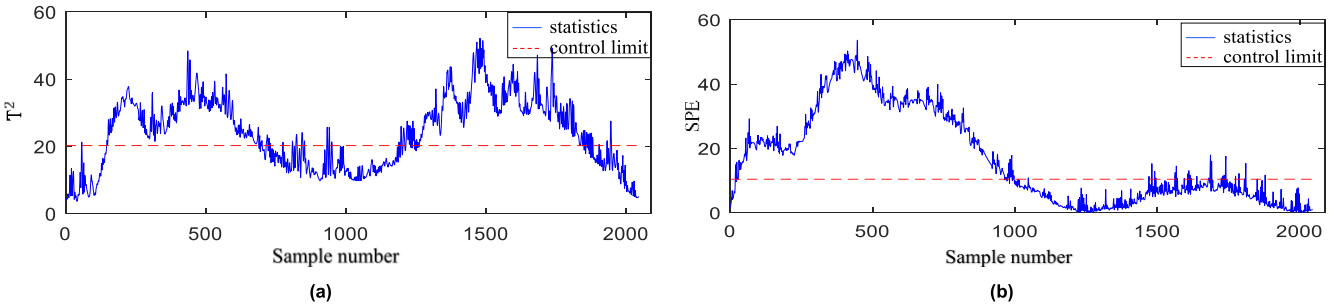

FIGURE 15. **Experimental results of PCA fault detection method for pitting faults.**

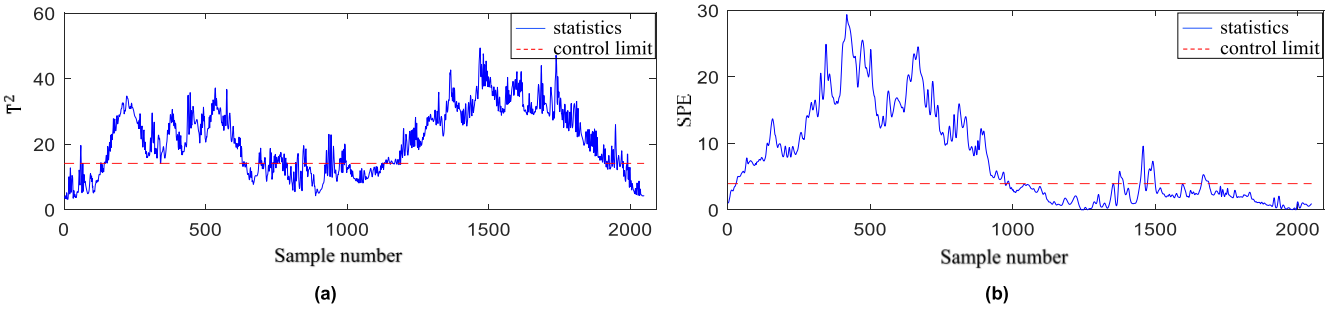

FIGURE 16. **Experimental results of DPCA fault detection method for pitting faults.**

The RDPCA method delays the detection of a failure at the 29th augmented data point, which is approximately at the 87th sampling point. The Deep PCA method detected failures at the 31st sampling point, and the Deep DPCA method delayed 28 sampling points. The Deep RDPCA method has a delay of eighth, that is, a failure is detected at about the 21st sampling point.

It can be seen that the amount of Deep RDPCA method can quickly detect the fault for the other five methods, and its missed detection rate is also the lowest among the six methods. In summary, Deep RDPCA has good fault detection performance.

B. GEARBOX PITTING FAILURE SIMULATION EXPERIMENT AND ANALYSIS

1) GEARBOX PITTING FAILURE SIMULATION EXPERIMENT

When the gear teeth enter the meshing, the tooth surface contact of the gear teeth under the action of the normal force will generate a large contact stress, and the contact stress will disappear after disengaging [38], [39]. For a fixed point on the working surface of the tooth profile, it is subject to contact stresses that are approximately pulsating. If the contact stress exceeds the contact fatigue limit of the gearbox material, irregular metal particles will peel off on the tooth surface and form pits. This phenomenon is called tooth surface fatigue pitting.

Pitting corrosion damages the working surface of the gear box, disrupts the normal operation of the gear box, causes unstable transmission and noise, and the gear tooth meshing situation will gradually deteriorate and be discarded [40]. In this section, a simulation experiment is performed on the gearbox with broken teeth. The specific results are as follows:

Fig. 15 and Fig. 16 describe the results of experiments on pitting faults based on PCA fault detection method and DPCA fault detection method. Among them, Fig. 15 (a) and Fig. 16(a) describe the results of the T^2 statistic detection, and Fig. 15 (b) and Fig. 16(b) describe the results of the SPE statistic detection. It can be seen from the simulation results that the missed detection rate of these two methods exceeds 50%, which shows that the traditional fault detection methods can hardly detect the incipient pitting faults.

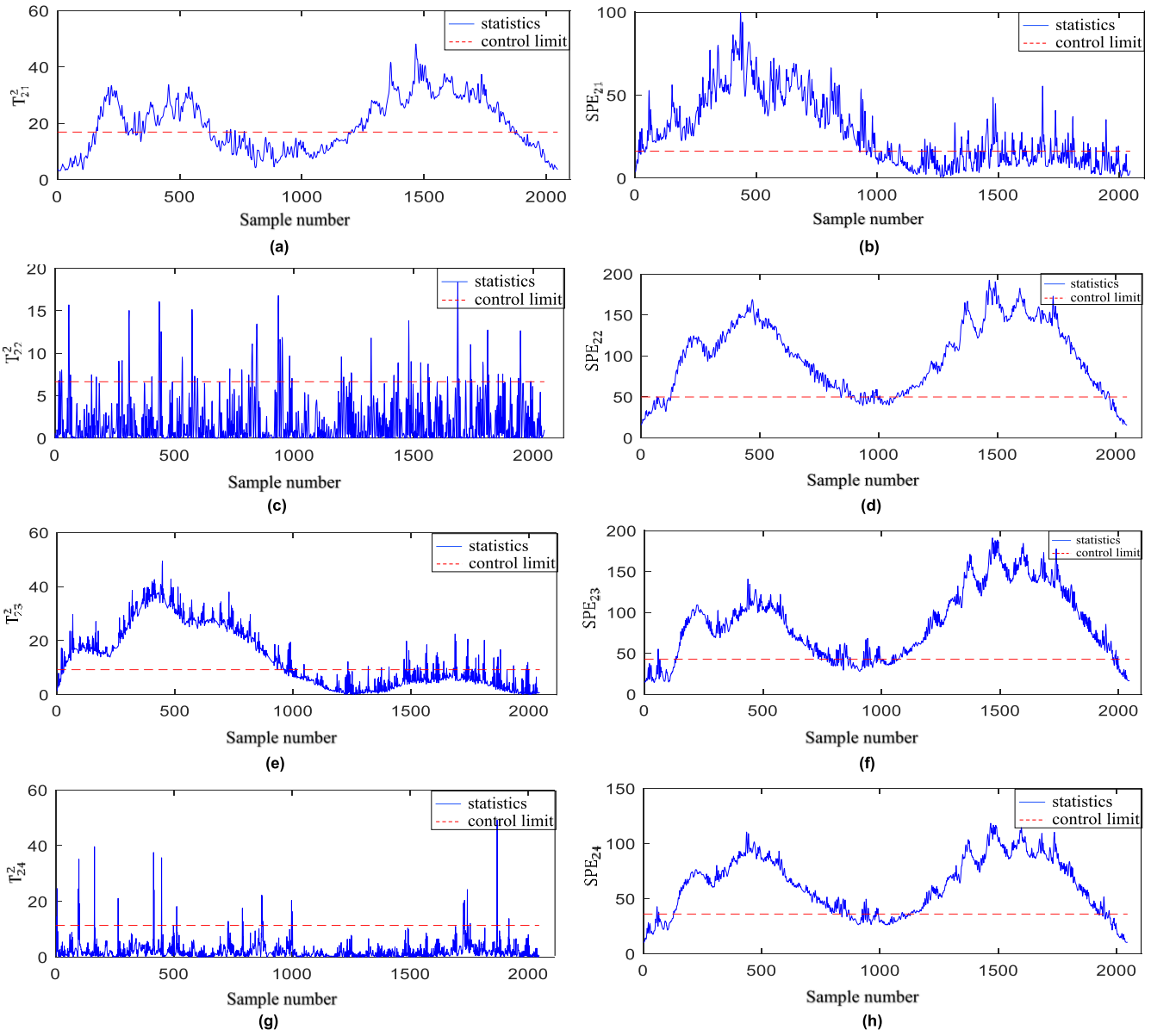

FIGURE 17. Experimental results of deep PCA fault detection method for pitting faults.

Fig. 17 (a)-(h) respectively describe the T^2 and SPE fault detection results of the third layer data set $X_{21} - X_{24}$ of gear pitting, based on Deep PCA method. Fig. 18 (a)-(h) respectively describe the T^2 and SPE fault detection results of the third layer data set $X_{21} - X_{24}$ of gear pitting, based on Deep DPCA method. Experimental results show that these two methods can detect the fault better, both of which are lower than 15%. At the same time, the fault detection effect of Deep DPCA is better than that of Deep PCA, because the Deep DPCA fault detection method takes into account the time-varying relationship of data.

Fig. 19 shows the results of pitting fault detection based on the Deep RDPCA fault detection method. Among them, Fig. 19(a) and Fig. 19(b) illustrate the detection result of the first layer data set X_{01}. Fig. 19(c)-(f) describe the result of the second layer data sets data set X_{11} and X_{12}. Fig. 19(g)-(n) describe the third layer data sets $X_{21} - X_{24}$. As can be seen from Fig. 19(a)-(f), we can obtain that, the affection of T_{01}^2, SPE_{01}, T_{11}^2, SPE_{11}, T_{12}^2 and SPE_{12} by this fault is small; In the Fig. 19(f), Fig. 19(l), Fig. 19(m) and Fig. 19(n), we can obtain that SPE_{22}, SPE_{23}, SPE_{24}, and T_{24}^2 are relatively affected by this fault, especially this fault has a very large impact on T_{24}^2, the missed detection rate is within 10%. Therefore, the effect on the third-layer of Deep RDPCA is better, which proves that this method is more sensitive to incipient failures.

2) PERFORMANCE COMPARISON

This part compares the experimental results of PCA, DPCA, RDPCA, Deep PCA, Deep DPCA, and Deep RDPCA by

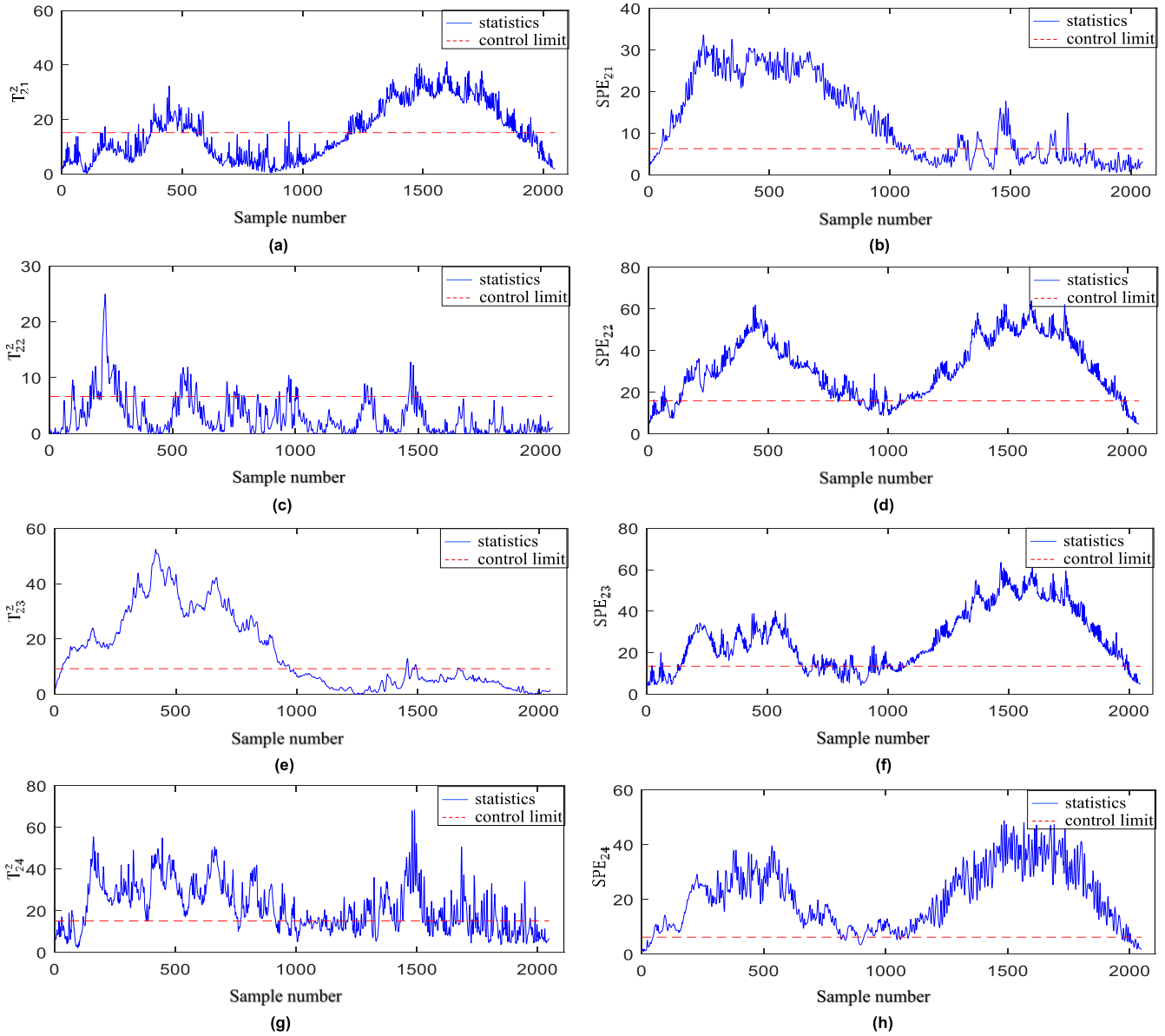

FIGURE 18. Experimental results of deep DPCA fault detection method for pitting faults.

analyzing the missed detection rate and detection delay of the gearbox pitting corrosion test results.

Table 2 describes the missed detection rates of the six methods for two types of pitting failures. From the perspective of missed detection rates, the PCA, DPCA, and RDPCA methods have a missed detection rates about 50%. The three methods basically do not have the capability of incipient fault detection. The missed detection rate of Deep PCA and Deep DPCA methods exceed 10%, significantly reduced compared to the PCA, DPCA and RDPCA methods, which can basically detect incipient failure. At the same time, compared with these two methods, the fault detection effect of Deep DPCA is better than that of Deep PCA. This is because Deep DPCA considers the time-varying of data. The missed detection rate of Deep RDPCA proposed in this paper is 7.14%,

TABLE 2. Gearbox pitting fault performance comparison.

Detection method	missed detection rate	detection delay
PCA	52.11%	64
DPCA	50.41%	63
RDPCA	48.65%	63
Deep PCA	12.19%	42
Deep DPCA	11.27%	37
Deep RDPCA	7.14%	12

respectively, and the detection effect is better than the other five methods.

From the perspective of detection delay, the PCA and DPCA methods detect failures at the 64th and 63th sampling points, respectively. The RDPCA method delay is the 21st augmented data point, that is, the failure is detected at the 63rd sampling point. The Deep PCA method detected a fault

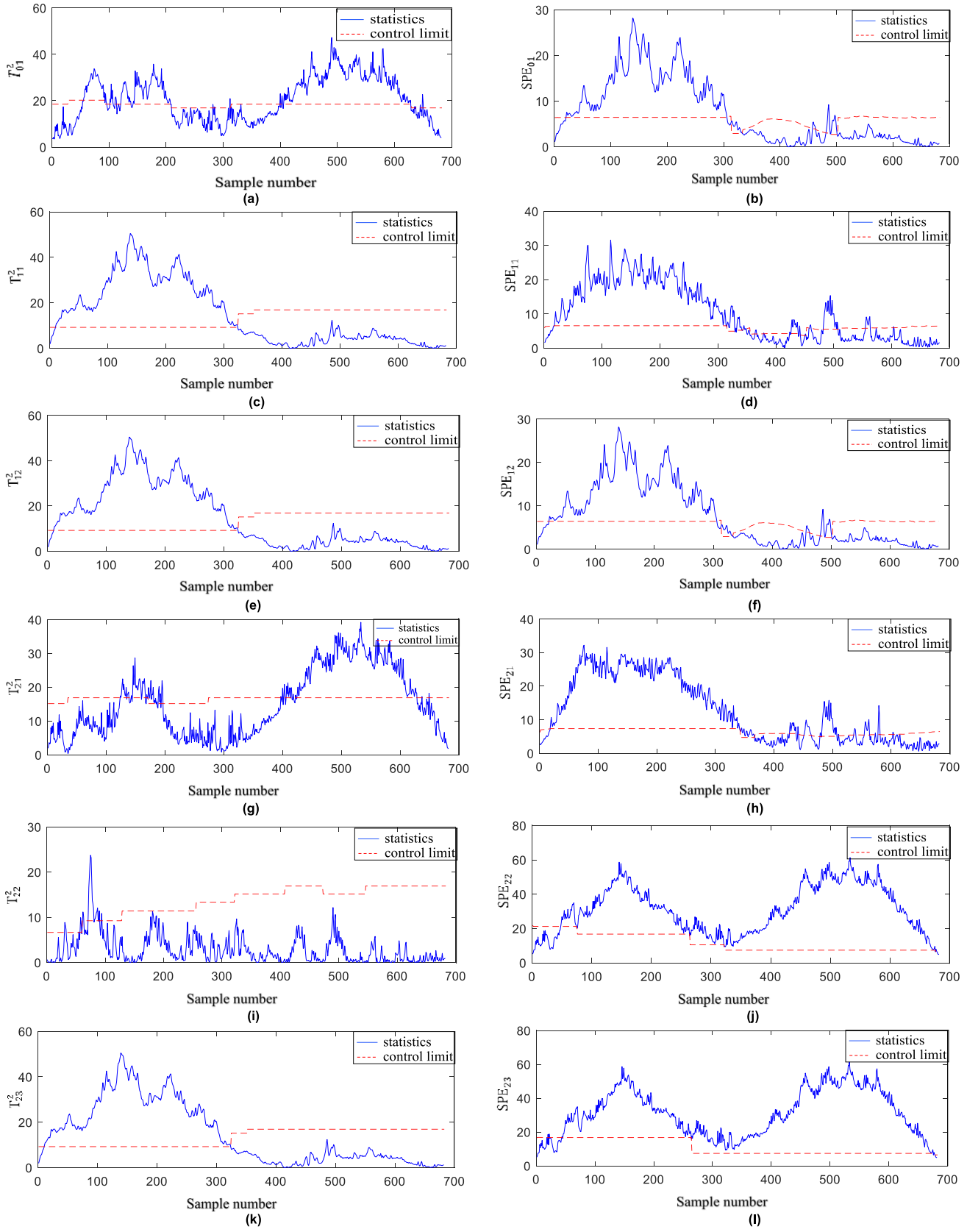

FIGURE 19. Experimental results of deep RDPCA fault detection method for pitting faults.

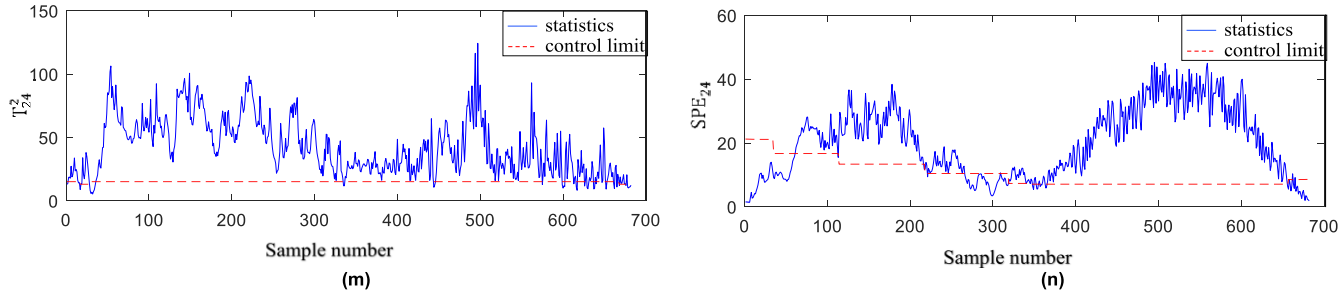

FIGURE 19. *(Continued.)* **Experimental results of deep RDPCA fault detection method for pitting faults.**

at the 42nd sampling point Although in the simulation results of pitting faults in this method, T^2_{24} detected the fault earlier, From the perspective of inspection rate, T^2_{24} is not sensitive to this fault, so determine the detection delay of this method from SPE_{23}. Deep DPCA method delay is 37 sampling point. The Deep RDPCA method has a delay of 4th, which is about 12nd sampling point. It can be seen that the Deep RDPCA method can quickly detect the fault for the other five methods. In summary, Deep RDPCA has good fault detection performance.

V. CONCLUSION

Aiming at early failures with insignificant failure characteristics, vibration signals with time-varying and unpredictable characteristics, this paper proposes a Deep RDPCA fault detection method. The following conclusions are obtained through theoretical analysis and experiments:

(1) The Deep RDPCA method considers the temporal correlation of data, and divides the data set more effectively. The problem of incipient fault characteristics is weak and the signal has time-varying is solved by Deep RDPCA method.

(2) This method combines the advantages of Deep PCA and Moving Window algorithm, effectively removes noise information and improves the incipient fault detection ability by capturing the timing relationship between variables. The feasibility of the method is proved by simulation experiments.

(3) Comparing with PCA, DPCA, RDPCA, Deep PCA, and Deep DPCA fault detection methods, the missed detection rate of Deep RDPCA fault detection method proposed in this paper less than 17%, lower than other methods. The detection delay time less than 24 sampling point. So the Deep RDPCA fault detection method has better incipient fault detection effect.

REFERENCES

[1] Y. Huangfu, K. Chen, H. Ma, X. Li, H. Han, and Z. Zhao, "Meshing and dynamic characteristics analysis of spalled gear systems: A theoretical and experimental study," *Mech. Syst. Signal Process.*, vol. 139, May 2020, Art. no. 106640, doi: 10.1016/j.ymssp.2020.106640.

[2] W. Hu, H. Chang, and X. Gu, "A novel fault diagnosis technique for wind turbine gearbox," *Appl. Soft Comput.*, vol. 82, Sep. 2019, Art. no. 105556, doi: 10.1016/j.asoc.2019.105556.

[3] J. Guo, Z. Shi, H. Li, D. Zhen, F. Gu, and A. Ball, "Early fault diagnosis for planetary gearbox based wavelet packet energy and modulation signal bispectrum analysis," *Sensors*, vol. 18, no. 9, p. 2908, Sep. 2018, doi: 10.3390/s18092908.

[4] C. Wang, H. Li, G. Huang, and J. Ou, "Early fault diagnosis for planetary gearbox based on adaptive parameter optimized VMD and singular kurtosis difference spectrum," *IEEE Access*, vol. 7, pp. 31501–31516, 2019, doi: 10.1109/ACCESS.2019.2903204.

[5] P. Cao, S. Zhang, and J. Tang, "Preprocessing-free gear fault diagnosis using small datasets with deep convolutional neural network-based transfer learning," *IEEE Access*, vol. 6, pp. 26241–26253, 2018, doi: 10.1109/ACCESS.2018.2837621.

[6] Z. Chen, C. Li, and R.-V. Sanchez, "Gearbox fault identification and classification with convolutional neural networks," *Shock Vibrat.*, vol. 2015, Oct. 2015, Art. no. 390134, doi: 10.1155/2015/390134.

[7] Y. Wei, M. Xu, X. Wang, W. Huang, and Y. Li, "A hybrid approach for weak fault feature extraction of gearbox," *IEEE Access*, vol. 7, pp. 16616–16625, 2019, doi: 10.1109/ACCESS.2018.2883536.

[8] Q. Li and S. Liang, "Weak fault detection for gearboxes using majorization–minimization and asymmetric convex penalty regularization," *Symmetry*, vol. 10, no. 7, p. 243, Jun. 2018, doi: 10.3390/sym10070243.

[9] Y. Li, M. Xu, Y. Wei, and W. Huang, "Health condition monitoring and early fault diagnosis of bearings using SDF and intrinsic characteristic-scale decomposition," *IEEE Trans. Instrum. Meas.*, vol. 65, no. 9, pp. 2174–2189, Sep. 2016, doi: 10.1109/TIM.2016.2564078.

[10] H. T. Shi and X. T. Bai, "Model-based uneven loading condition monitoring of full ceramic ball bearings in starved lubrication," *Mech. Syst. Signal Process.*, vol. 139, May 2020, Art. no. 106583, doi: 10.1016/j.ymssp.2019.106583.

[11] S. Ji, H. Cao, J. Zhao, Y. Pan, and E. Jiang, "Soft abrasive flow polishing based on the cavitation effect," *Int. J. Adv. Manuf. Technol.*, no. 101, pp. 1865–1878. Apr. 2019, doi: 10.1007/s00170-018-2983-9.

[12] A. B. Zoubi, S. Kim, D. O. Adams, and V. J. Mathews, "Lamb wave mode decomposition based on cross-Wigner-Ville distribution and its application to anomaly imaging for structural health monitoring," *IEEE Trans. Ultrason., Ferroelectr., Freq. Control*, vol. 66, no. 5, pp. 984–997, May 2019, doi: 10.1109/tuffc.2019.2903006.

[13] L. Tang and D. Li, "Time-varying barrier Lyapunov function based adaptive neural controller design for nonlinear pure-feedback systems with unknown hysteresis," *Int. J. Control, Autom. Syst.*, vol. 17, no. 7, pp. 1642–1654, Jul. 2019, doi: 10.1007/s12555-018-0745-y.

[14] H. T. Shi, X. T. Bai, K. Zhang, Y. H. Wu, and G. D. Yue, "Influence of uneven loading condition on the sound radiation of starved lubricated full ceramic ball bearings," *J. Sound Vib.*, vol. 461, Nov. 2019, Art. no. 114910, doi: 10.1016/j.jsv.2019.114910.

[15] Y. Liu, Y. L. Zhao, J. T. Li, H. Ma, Q. Yang, and X. X. Yan, "Application of weighted contribution rate of nonlinear output frequency response functions to rotor rub-impact," *Mech. Syst. Signal Process.*, vol. 136, Feb. 2020, Art. no. 106518, doi: 10.1016/j.ymssp.2019.106518.

[16] G. Li, G. Tang, G. Luo, and H. Wang, "Underdetermined blind separation of bearing faults in hyperplane space with variational mode decomposition," *Mech. Syst. Signal Process.*, vol. 120, pp. 83–97, Apr. 2019, doi: 10.1016/j.ymssp.2018.10.016.

[17] L. Cui, X. Wang, H. Wang, and J. Ma, "Research on remaining useful life prediction of rolling element bearings based on time-varying Kalman filter," *IEEE Trans. Instrum. Meas.*, early access, Jul. 8, 2019, doi: 10.1109/TIM.2019.2924509.

[18] Y. Li, M. Xu, X. Liang, and W. Huang, "Application of bandwidth EMD and adaptive multiscale morphology analysis for incipient fault diagnosis of rolling bearings," *IEEE Trans. Ind. Electron.*, vol. 64, no. 8, pp. 6506–6517, Aug. 2017, doi: 10.1109/TIE.2017.2650873.

[19] D. Wang and K.-L. Tsui, "Dynamic Bayesian wavelet transform: New methodology for extraction of repetitive transients," *Mech. Syst. Signal Process.*, vol. 88, pp. 137–144, May 2017, doi: 10.1016/j.ymssp.2016.11.003.
[20] Y. Wang, P. W. Tse, B. Tang, Y. Qin, L. Deng, and T. Huang, "Kurtogram manifold learning and its application to rolling bearing weak signal detection," *Measurement*, vol. 127, pp. 533–545, Oct. 2018, doi: 10.1016/j.measurement.2018.06.026.
[21] X. Wang, Y. Qin, Y. Wang, S. Xiang, and H. Chen, "ReLTanh: An activation function with vanishing gradient resistance for SAE-based DNNs and its application to rotating machinery fault diagnosis," *Neurocomputing*, vol. 363, pp. 88–98, Oct. 2019, doi: 10.1016/j.neucom.2019.07.017.
[22] Y. Qin, S. Xiang, Y. Chai, and H. Chen, "Macroscopic-microscopic attention in LSTM networks based on fusion features for gear remaining life prediction," *IEEE Trans. Ind. Electron.*, early access, Dec. 18, 2019, doi: 10.1109/TIE.2019.2959492.
[23] D. F. Wang, Y. Guo, X. Wu, J. Na, and G. Litak, "Planetary-gearbox fault classification by convolutional neural network and recurrence plot," *Appl. Sci.*, vol. 10, no. 3, Jan. 2020, Art. no. 932, doi: 10.3390/app10030932.
[24] H. Shi, L. Guo, S. Tan, and X. Bai, "Rolling bearing initial fault detection using long short-term memory recurrent network," *IEEE Access*, vol. 7, pp. 171559–171569, 2019, doi: 10.1109/ACCESS.2019.2954091.
[25] A. Stief, J. R. Ottewill, J. Baranowski, and M. Orkisz, "A PCA and two-stage Bayesian sensor fusion approach for diagnosing electrical and mechanical faults in induction motors," *IEEE Trans. Ind. Electron.*, vol. 66, no. 12, pp. 9510–9520, Dec. 2019, doi: 10.1109/TIE.2019.2891453.
[26] G. Li and Y. Hu, "An enhanced PCA-based chiller sensor fault detection method using ensemble empirical mode decomposition based denoising," *Energy Buildings*, vol. 183, pp. 311–324, Jan. 2019, doi: 10.1016/j.enbuild.2018.10.013.
[27] H. Chen, B. Jiang, N. Lu, and Z. Mao, "Deep PCA based real-time incipient fault detection and diagnosis methodology for electrical drive in high-speed trains," *IEEE Trans. Veh. Technol.*, vol. 67, no. 6, pp. 4819–4830, Jun. 2018, doi: 10.1109/TVT.2018.2818538.
[28] L. Tang, D. Ma, and J. Zhao, "Adaptive neural control for switched non-linear systems with multiple tracking error constraints," *IET Signal Process.*, vol. 13, no. 3, pp. 330–337, May 2019, doi: 10.1049/iet-spr.2018.5077.
[29] Q. Zhang, J. Wang, P. Lin, and L. Hou, "Application of an improved DPCA algorithm in rock-fall monitoring based on synthetic aperture radar," *Natural Hazards*, vol. 94, no. 3, pp. 1043–1055, Dec. 2018, doi: 10.1007/s11069-018-3454-1.
[30] L. Liu, Y.-J. Liu, D. Li, S. Tong, and Z. Wang, "Barrier Lyapunov function-based adaptive fuzzy FTC for switched systems and its applications to Resistance-Inductance-Capacitance circuit system," *IEEE Trans. Cybern.*, early access, Aug. 16, 2019, doi: 10.1109/TCYB.2019.2931770.
[31] L. Tang, A. Chen, and D. Li, "Time-varying tan-type barrier Lyapunov function-based adaptive fuzzy control for switched systems with unknown dead zone," *IEEE Access*, vol. 7, pp. 110928–110935, 2019, doi: 10.1109/ACCESS.2019.2934117.
[32] W. Ku, R. H. Storer, and C. Georgakis, "Disturbance detection and isolation by dynamic principal component analysis," *Chemometrics Intell. Lab. Syst.*, vol. 30, no. 1, pp. 179–196, Nov. 1995, doi: 10.1016/0169-7439(95)00076-3.
[33] C. Zhang, Q. Guo, and Y. Li, "Fault detection method based on principal component difference associated with DPCA," *J. Chemometrics*, vol. 33, no. 1, Jan. 2019, Art. no. e3082, doi: 10.1002/cem.3082.
[34] K. Song, P. Xu, Y. Chen, T. Zhang, G. Wei, and Q. Wang, "A fault diagnosis and reconfiguration strategy for self-validating hydrogen sensor array based on MWPCA and ELM," *IEEE Access*, vol. 7, pp. 115075–115092, 2019, doi: 10.1109/ACCESS.2019.2936128.
[35] H. Ma, J. Zeng, R. Feng, X. Pang, Q. Wang, and B. Wen, "Review on dynamics of cracked gear systems," *Eng. Failure Anal.*, vol. 55, pp. 224–245, Sep. 2015, doi: 10.1016/j.engfailanal.2015.06.004.
[36] L. S. Dhamande and M. B. Chaudhari, "Compound gear-bearing fault feature extraction using statistical features based on time-frequency method," *Measurement*, vol. 125, pp. 63–77, Sep. 2018, doi: 10.1016/j.measurement.2018.04.059.
[37] X. Liang, M. J. Zuo, and L. Liu, "A windowing and mapping strategy for gear tooth fault detection of a planetary gearbox," *Mech. Syst. Signal Process.*, vol. 80, pp. 445–459, Dec. 2016, doi: 10.1016/j.ymssp.2016.04.034.
[38] R. Medina, M. Cerrada, D. Cabrera, R.-V. Sanchez, C. Li, and J. V. D. Oliveira, "Deep learning-based gear pitting severity assessment using acoustic emission, vibration and currents signals," in *Proc. Prognostics Syst. Health Manage. Conf. (PHM-Paris)*, May 2019, pp. 210–216, doi: 10.1109/PHM-Paris.2019.00042.
[39] J. Kattelus, J. Miettinen, and A. Lehtovaara, "Detection of gear pitting failure progression with on-line particle monitoring," *Tribol. Int.*, vol. 118, pp. 458–464, Feb. 2018, doi: 10.1016/j.triboint.2017.02.045.
[40] X. Li, J. Li, Y. Qu, and D. He, "Gear pitting fault diagnosis using integrated CNN and GRU network with both vibration and acoustic emission signals," *Appl. Sci.*, vol. 9, no. 4, Feb. 2019, Art. no. 768, doi: 10.3390/app9040768.

HUAITAO SHI received the B.S. and Ph.D. degrees in control engineering from Northeastern University, Shenyang, China, in 2005 and 2012, respectively. He has been a Professor with the Faculty of Mechanical Engineering, Shenyang Jianzhu University, Shenyang, where he has been the Vice Dean, since 2014. He is the author of more than 30 articles, (16 articles were indexed by SCI), and five patents. His current research interest includes hybrid ceramic ball-bearing.

JIN GUO was born in Liaoning, China, in 1996. She received the B.S. degree in industrial engineering from Shenyang Aerospace University, Shenyang, China, in 2018. She is currently pursuing the M.S. degree in mechanical engineering from Shenyang Jianzhu University. Her current research interest includes fault detection and diagnosis.

XIAOTIAN BAI was born in Fushun, Liaoning, China, in 1989. He received the B.S. degree in mechanical engineering from the Dalian University of Technology, Dalian, in 2011, and the M.S. and Ph.D. degrees in mechanical engineering from the Shenyang University of Technology in 2013 and 2016, respectively.

He has been a Lecturer with the Faculty of Mechanical Engineering, Shenyang Jianzhu University, Shenyang, Liaoning, China, since 2016. He carried out his Postdoctoral work at the Postdoctoral Station, Shenyang Jianzhu University, from 2016 to 2018. He was a Visiting Scholar in Romania for three months. He is the author of over 15 articles. He holds over two patents. His current research interest includes vibration and sound radiation of bearings.

LEI GUO was born in 1994. He received the B.S. degree in mechanical design manufacture and automation from Jiamusi University, China, in 2017. He is currently pursuing the M.S. degree in mechanical engineering from Shenyang Jianzhu University. His research interest includes faults detection of mechanical systems.

ZHENPENG LIU, photograph and biography not available at the time of publication.

JIE SUN, photograph and biography not available at the time of publication.